An Investigation of the Opacity of High-Z Mixtures and Implications for ICF Hohlraum Design

P. Wang, J.J. MacFarlane, T.J. Orzechowski

May 1996

UWFDM-1012

Presented at the 11th Topical Conference on High-Temperature Plasma Diagnostics, Monterey, CA, 12–16 May 1996; to be published in *Review of Scientific Instruments*.

FUSION TECHNOLOGY INSTITUTE

UNIVERSITY OF WISCONSIN

MADISON WISCONSIN

An Investigation of the Opacity of High-Z Mixtures and Implications for ICF Hohlraum Design

P. Wang and J. J. MacFarlane

Fusion Technology Institute
Department of Nuclear Engineering and Engineering Physics
University of Wisconsin-Madison
Madison, WI 53706

T. J. Orzechowski

Lawrence Livermore National Laboratory
Livermore, CA 94550

May 1996

UWFDM-1012

Presented at the 11th Topical Conference on High-Temperature Plasma Diagnostics, Monterey, CA, 12–16 May 1996; to be published in *Review of Scientific Instruments*.

Abstract

We use an Unresolved Transition Array (UTA) model to investigate the opacities of high-Z materials and their mixtures which are of interest to indirect-drive ICF hohlraum design. In particular, we report on calculated opacities for pure Au, Gd, Sm, as well as Au-Sm, and Au-Gd mixtures. Our results indicate that mixtures of Au-Gd and Au-Sm can produce a significant enhancement in the Rosseland mean opacity. Radiation-hydrodynamics simulations of Au radiation burnthrough are also presented, and compared with NOVA experimental data.

I. Introduction

High-Z materials are of great interest in indirect-drive ICF hohlraum design because of their high reemission and x-ray conversion efficiency. It has been proposed[1] that using a mixture of two high-Z elements, such as gold and another metallic element in the lanthanide series, can provide significantly higher Rosseland mean opacities and albedos than those of pure elements. This occurs when the major absorption valleys (i.e., frequency regions of small opacity) of one element coincide with the absorption peaks of another element in the same photon energy band. Gold has been the most widely used material for ICF hohlraum fabrication. To select the optimum element to mix with gold, it is necessary to accurately determine the major absorption peaks and valleys for each high-Z species over the temperature and density range of interest. As temperature and density conditions vary, the ionization distribution changes, resulting in shifts in the frequency-dependent absorption. A suitable candidate for mixing with gold will provide a higher opacity in photon energy bands where the gold opacity is relatively low. In this work, we investigate the opacity characteristics of pure gold in the density range of 0.01 g/cm^3 to 20 g/cm^3 and temperature range of 50 eV to 300 eV, which are relavant to NOVA and NIF hohlraum plasmas. We also investigate the enhancement of the Rosseland mean opacity of Au-Sm and Au-Gd mixtures.

II. Opacity Calculations for High-Z Materials

The calculation of opacities for high-Z, as well as low-Z, plasmas requires models for computing atomic structure, level populations, radiative transition cross sections, spectral line shapes, and plasma effects. However, the atomic structure of high-Z atomic systems is much more complicated due to many electronic configurations with open d and f shells. Due to angular momentum coupling, configurations of this kind can have hundreds, or even thousands, of levels. The possible transitions between these levels are so

numerous that it is impractical to use a detailed term accounting (DTA) model, which is a standard approach used for low-Z atomic systems. On the other hand, the term splitting in high-Z atomic systems significantly affects the opacities. In our calculations, we use a detailed configuration accounting (DCA) method, but with term splitting effects included using an unresolved transition array (UTA) model assuming $j-j$ coupling.[2] The UTA model treats the superposition of many overlapping, intrinsically broadened bound-bound transitions resulting from two electronic configurations as a single spectral feature. Each configuration-configuration transition array is then characterized by average quantities such as total intensity, average transition energy, and variance. In our calculations, the transition energies, oscillator strengths, and variances are evaluated using Dirac-Fock-Slater[3,4] self-consistent field potentials. Atomic configuration populations are calculated assuming local thermodynamic equilibrium (LTE).

To test the accuracy of our UTA opacity calculations we have compared our calculated absorption spectra for iron and germanium to experimental data.[5,6] Figure 1 shows our calculated absorption spectra for Fe at $T = 59$ eV, $\rho = 0.0127$ g/cm^3, areal density of 272 μg/cm^2 (top), and Ge at $T = 76$ eV, $\rho = 0.05$ g/cm^3, and areal density of 160 μg/cm^2. These are the experimentally determined plasma conditions.[5,6] It can be seen that our UTA calculations are in good agreement with the observed spectra in both cases. The calculated Rosseland and Planck mean opacities for iron are $\overline{\chi_R} = 4377$ cm^2/g and $\overline{\chi_P} = 8459$ cm^2/g. These are also in good agreement with the experimental results, which are 4400 ± 600 cm^2/g and 8200 ± 700 cm^2/g, respectively. This favorable comparison with experimental data for the intermediate-Z plasmas gives us the confidence that our UTA opacity calculation for high-Z plasmas should be reasonably accurate.

To study the opacity characteristics of pure gold, we have examined the spectra of the monochromatic opacity for gold over the temperature and density range of our interest. In particular, we identify all the dominant absorption features and valleys and determine

their relative contributions to the Rosseland mean opacity. A quantitative indicator used in our opacity analysis is the ratio of the *accumulated* Rosseland mean, defined as:

$$\overline{\chi_R^{-1}}(\nu) = \left(\frac{\pi}{4\sigma_R T^3}\right) \int_0^{\nu} \kappa_{\nu'}^{-1} \left(\frac{dB_{\nu'}}{dT}\right) d\nu' \,, \tag{1}$$

to the *total* Rosseland mean

$$\overline{\chi_R^{-1}} = \left(\frac{\pi}{4\sigma_R T^3}\right) \int_0^{\infty} \kappa_{\nu'}^{-1} \left(\frac{dB_{\nu'}}{dT}\right) d\nu' \,, \tag{2}$$

where σ_R is Stefan-Boltzmann constant and B_ν is the Planck function. Note that the integral is evaluated from 0 to ν in Eq. (1), while it is evaluated from 0 to ∞ in Eq. (2). The ratio provides an indication of the relative contribution of different frequency regions to the Rosseland mean opacity.

For a Au plasma at $T = 200$ eV and $\rho = 0.1$ g/cm^3, the average charge state is 34, with the dominant ions ranging from Nb-like to Ag-like. The major features in the corresponding absorption spectrum include: (1) strong absorption features resulting from $4d \rightarrow 4f$ and $4p \rightarrow 4d$ transitions; (2) an absorption valley caused by the gap between the transitions of $n = 4 \rightarrow n = 4$ and $n = 4 \rightarrow n > 4$; (3) absorption features corresponding to the transitions $n = 4 \rightarrow n > 4$; (4) an absorption valley between the N-band and M-band; (5) a strong absorption feature arising from $3d \rightarrow 4f$ transitions; and (6) additional M-band absorption features ($n = 3 \rightarrow n \geq 4$).

For other temperature and density conditions considered here, although the relative strengths of the different absorption features and the depth and width of absorption valleys change, two major absorption valleys near regions 2 and 4 are seen in all cases. Because the Rosseland mean opacity is a harmonic mean, it is most sensitive to regions of low absorption. We find that these two major absorption valleys (regions 2 and 4) make up approximately 80% of the total Rosseland mean. If these two absorption valleys can be smeared out by mixing gold with another high-Z element, one can expect to see a

significant increase in the Rosseland mean opacity. Thus, it is of value to identify other high-Z species whose opacities are relatively high at these photon energies.

III. The Opacity of High-Z Mixtures

In calculating opacities for high-Z mixtures, we compute the equilibrium occupation numbers by solving the Saha equation including all the levels of both species in the mixture. Thus, plasma effects on both elements are consistent with the conditions of the mixture plasma.

Examination of the basic atomic structure data for the elements on the lanthanide series indicates that the transition energies of the major absorption peaks of these elements are about forty to fifty percent smaller than those of the corresponding transitions in gold. These major absorption peaks roughly lay in the regions where major absorption valleys of gold appear. One can therefore expect that an enhancement in Rosseland mean opacity can be achieved by mixing gold with one of these elements. Our calculations show that in a wide range of temperature and density conditions, the major absorption peaks of Sm and Gd ($n = 3 \rightarrow n > 3$ near 1-2 keV and $n = 4 \rightarrow n > 4$ near 0.3-0.7 keV) nicely fill in the two major absorption valleys of gold, and therefore result in significant enhancement of the Rosseland mean opacity. For example, we find almost a factor of two increase in Rosseland mean opacity for a Au-Sm mixture with a 1:1 particle number mixing ratio at T=225 eV and $\rho = 0.1$ g/cm^3.

To study the Rosseland mean opacity enhancement effect of high-Z mixtures, we have performed a series of opacity calculations for mixtures of Au-Sm and Au-Gd with various mixing ratios over a range of temperature and density conditions relevant to ICF hohlraums. Some typical results are shown in Figure 2. In this figure, the Rosseland mean opacities for Au-Sm and Au-Gd mixtures are plotted as a function of the fractional number density of gold at the density of 0.1 g/cm^3, and at four different temperatures ranging from

150 eV to 300 eV. It is seen that the Rosseland mean opacity is significantly enhanced in the Au-Sm and Au-Gd mixtures. Note also that the enhancements are sensitive to the plasma temperatures.

This temperature dependence can be seen more clearly from Figure 3, where the Rosseland mean opacities of Au, Sm, and a Au-Sm mixture are shown as a function of temperature. An interesting feature of the Au curve is that the Rosseland mean opacity exhibits a plateau near $T = 185$ eV. The Sm Rosseland mean opacity also exhibits a plateau near $T = 350$ eV. The Au-Sm mixture produces the most significant enhancement for the Rosseland mean opacity at temperatures from about 200 to 400 eV; that is, where the Au and Sm opacities are comparable. This temperature dependence has to do with changes in the ionization distribution. We find that as the temperature increases from 100 eV to 300 eV, the average charge state of gold increases from 23 to 43. As shown in Figure 4, for temperatures below about 185 eV, the configurations with $4f$ electrons are highly populated, and the major absorption features caused by $4f \rightarrow 5g$ and $4f \rightarrow 5d$ transitions are very strong. The existence of these two absorption features reduces the width of the absorption valley in the 400 eV spectral region which is heavily weighted in computing the Rosseland mean opacity. The Rosseland mean opacity does not show significant temperature dependence until the $4f$ electrons disappear from the most populated states. Therefore, we see a Rosseland mean opacity plateau near $T = 185$ eV. As the temperature increases above 200 eV, the $4f \rightarrow 5g$ and $4f \rightarrow 5d$ absorption features are dramatically reduced due to a depopulation of the $4f$ subshell. This causes the absorption valley in the spectral region of 400 eV to widen, producing a significant decrease in the Au Rosseland mean opacity. In Au-Sm or Au-Gd mixtures, however, this absorption valley is effectively filled in by the absorption features arising from $n = 4 \rightarrow n > 4$ transitions of Sm or Gd. Hence, as the temperature increases the Rosseland mean opacity of the mixtures decreases, but less so than for pure gold.

To test the reliability of our UTA opacities for Au, we have performed simulations of Au radiation burnthrough experiments performed at NOVA.[7] The calculations were performed using BUCKY-1,[8] which is a 1-D Lagrangian radiation-hydrodynamics code. In these simulations, a multiangle radiation transport model was used with 100 frequency groups. A time-dependent radiation temperature boundary condition (with a Planckian spectrum) was applied to one side of the Au. The peak radiation temperature of 252 eV used in the simulation is consistent with the "wall temperature" measured by DANTE[7] and assumes an albedo of 0.8. Figure 5 shows a comparison of the calculated rear side fluxes for 1 and 2 μm-thick foils (top) with experimental x-ray streak camera data (bottom). For both foil thicknesses, good agreement is found in the times at which the x-ray wave burns through the Au foils, suggesting that our UTA opacity model should be reasonably accurate.

IV. Summary

Using an Unresolved Transition Array (UTA) model and relativistic self-consistent-field atomic data, we have investigated the opacity characteristics of high-Z materials and several mixtures. We have found that in temperature and density regimes relevant to ICF hohlraum plasmas, there are two major absorption valleys in gold which significantly affect the Rosseland mean opacity. These absorption valleys can be filled in significantly by mixing Au with either Sm or Gd. The Rosseland mean opacities of the Au-Sm and Au-Gd mixtures are found to be notably higher than that of pure Au. The enhancements for Au-Sm are predicted to be somewhat higher than those for Au-Gd at a given temperature.

Acknowledgement

This work is supported in part by Lawrence Livermore National Laboratories under U.S. Department of Energy Contract No. W-7405-ENG-48.

References

1. H. Nishimura, T. Endo, H. Shiraga, Y. Kato, and S. Nakai, *Appl. Phys. Lett.* **62**, 1344 (1993).

2. C. Bauche-Arnoult, J. Bauche, and M. Klapisch, *J. Opt. Soc. Am.* **68**, 1136 (1978); C. Bauche-Arnoult, J. Bauche, and M. Klapisch, *Adv. At. Mol. Phys.* **23**, 131 (1988).

3. D.A. Liberman, D. T. Cromer, and J. T. Waber, *Comput. Phys. Commun.* **2**, 107 (1971).

4. D. H. Sampson, H. L. Zhang, A. K. Mohanty, and R. E. Clark, *Phys. Rev.* **40**, 604 (1989).

5. P. T. Springer, D. J. Fields, B. G. Wilson, J. K. Nash, W. H. Goldstein, C. A. Iglesias, F. J. Rogers, J. K. Swenson, M. H. Chen, A. Bar-Shalom, and R. E. Steward, *Phys. Rev. Lett.* **69(26)**, 3735 (1992).

6. J. M. Foster, D. J. Hoarty, C. C. Smith, P. A. Rosen, and Sl J. Davidson, S. J. Rose, T. S. Perry and F.J.D. Zerduke, *Phys. Rev. Lett.* **67(23)**, 3255 (1991).

7. J. L. Porter, T. J. Orzechowski, M. D. Rosen, A. R. Thiessen, L. J. Suter, and J. T. Larsen, Lawrence Livermore National Laboratory ICF Quarterly Report, UCRL-LR-105821-94-4 (1994).

8. J. J. MacFarlane, G. A. Moses, and R. R. Peterson, "BUCKY-1 – A 1-D Radiation-Hydrodynamics Code for Simulating Inertial Confinement Fusion High Energy Density Plasmas," University of Wisconsin Fusion Technology Institute Report UWFDM-984 (August 1995).

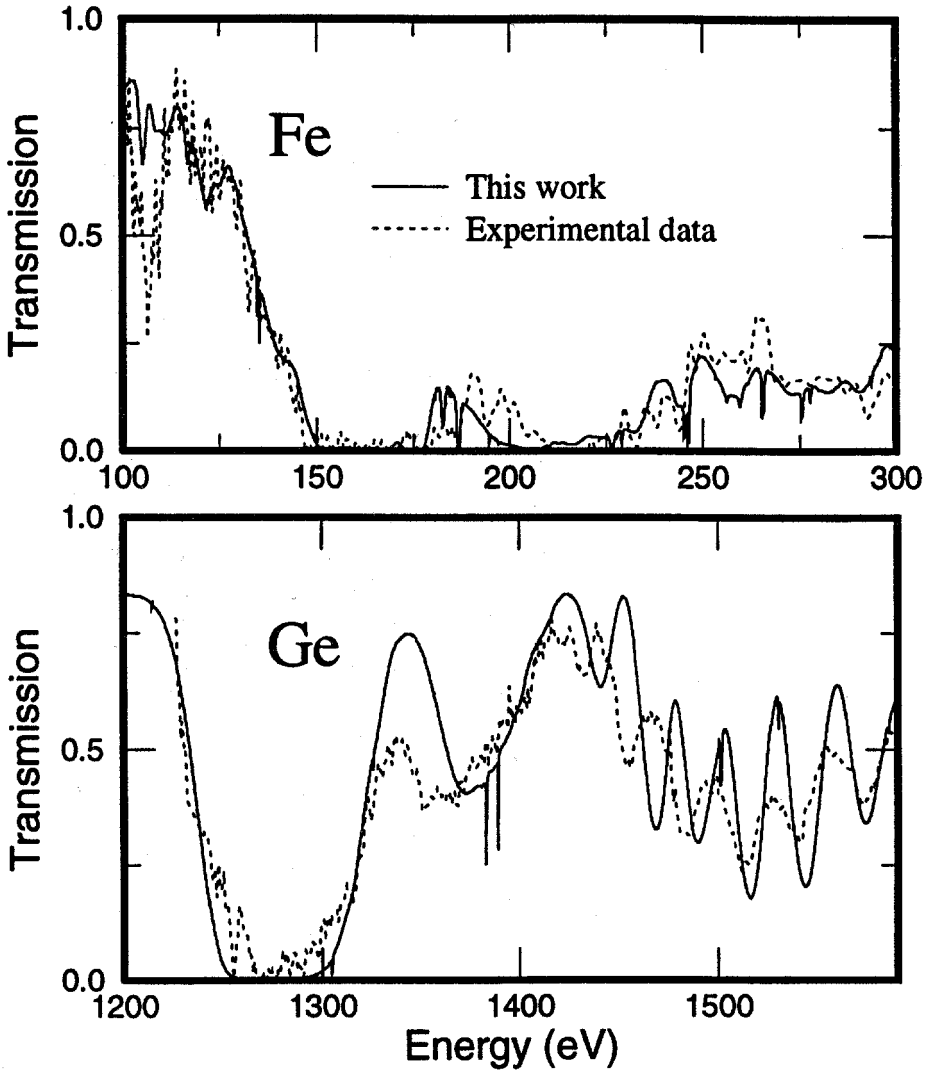

Figure 1. (Top) Comparison of experimental transmission data (dotted line) and calculations for an iron plasma of $\rho = 1.27 \times 10^{-2}$ g/cm^3, $T = 59$ eV, and areal density of 272 μg cm^{-2}. (Bottom) Same for a germanium plasma of $\rho = 0.05$ g/cm^3, $T = 76$ eV, and areal density of 160 μg cm^{-2}.

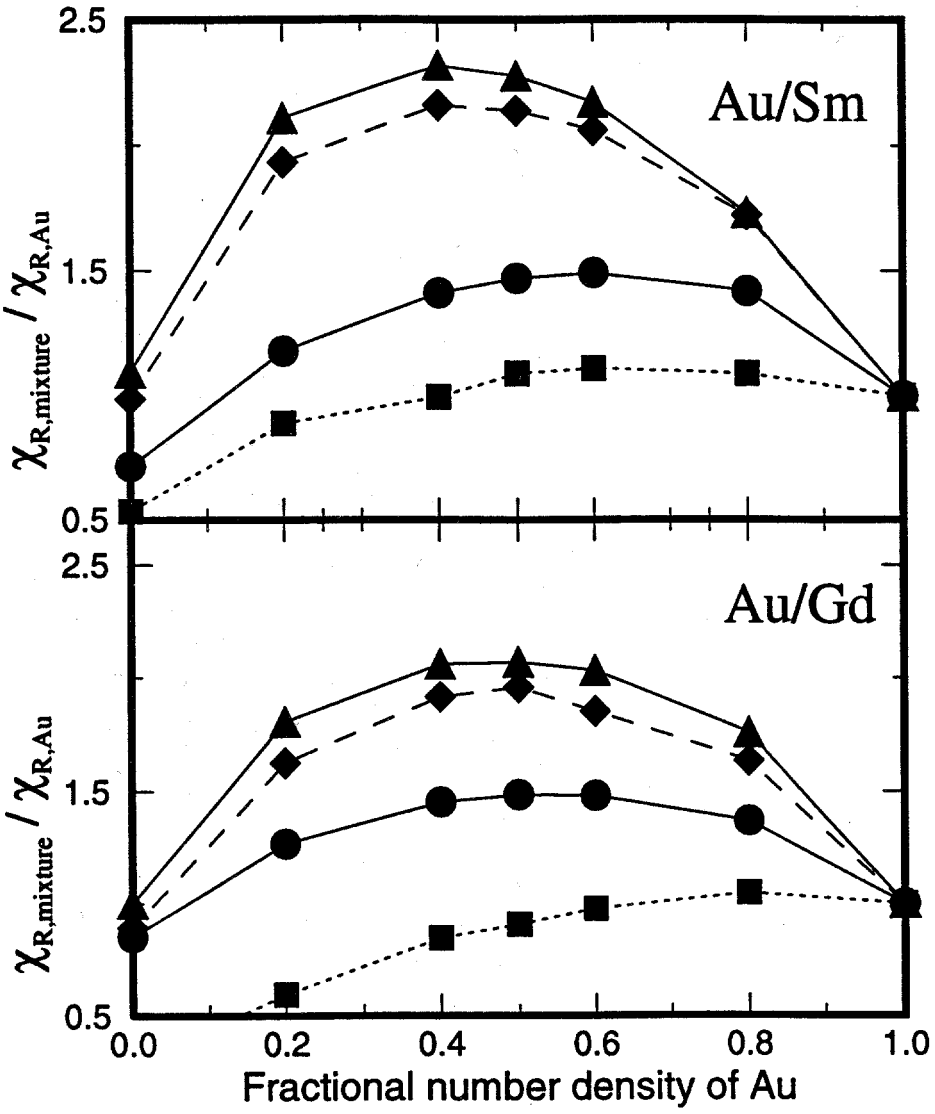

Figure 2. Calculated Rosseland mean opacity for Au-Sm and Au-Gd mixtures vs. fractional number density of gold. The density of the mixtures for both Au-Sm and Au-Gd is 0.1 g/cm^3. Results of four different temperatures are shown, and the Rosseland mean opacities for mixtures are scaled to the corresponding Au values: $T = 150$ eV (circles), $\chi_{R,Au} = 2158$ cm^2/g; $T = 200$ eV (squares), $\chi_{R,Au} = 1045$ cm^2/g; $T = 250$ eV (diamonds),$\chi_{R,Au} = 570$ cm^2/g; and $T = 300$ eV (triangles), $\chi_{R,Au} = 440$ cm^2/g.

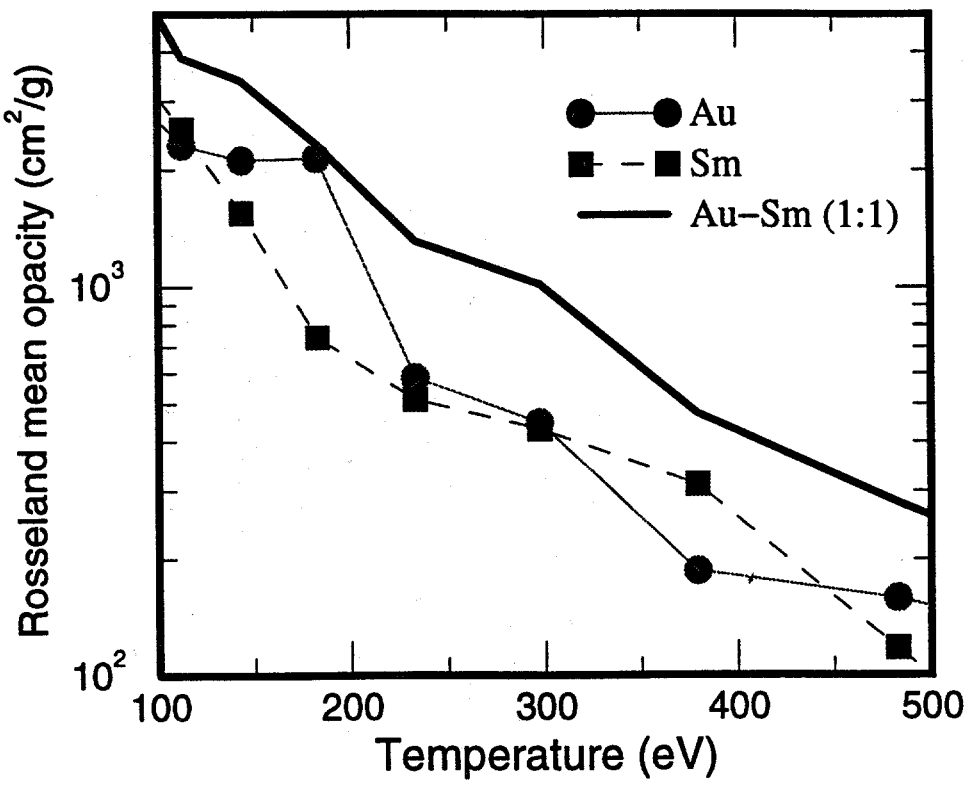

Figure 3. Calculated Rosseland mean opacities for Au, Sm, and a Au-Sm mixture as a function of plasma temperature. The density of the plasma is 0.1 g/cm^3. The particle number mixing ratio for the Au-Sm mixture is 1:1.

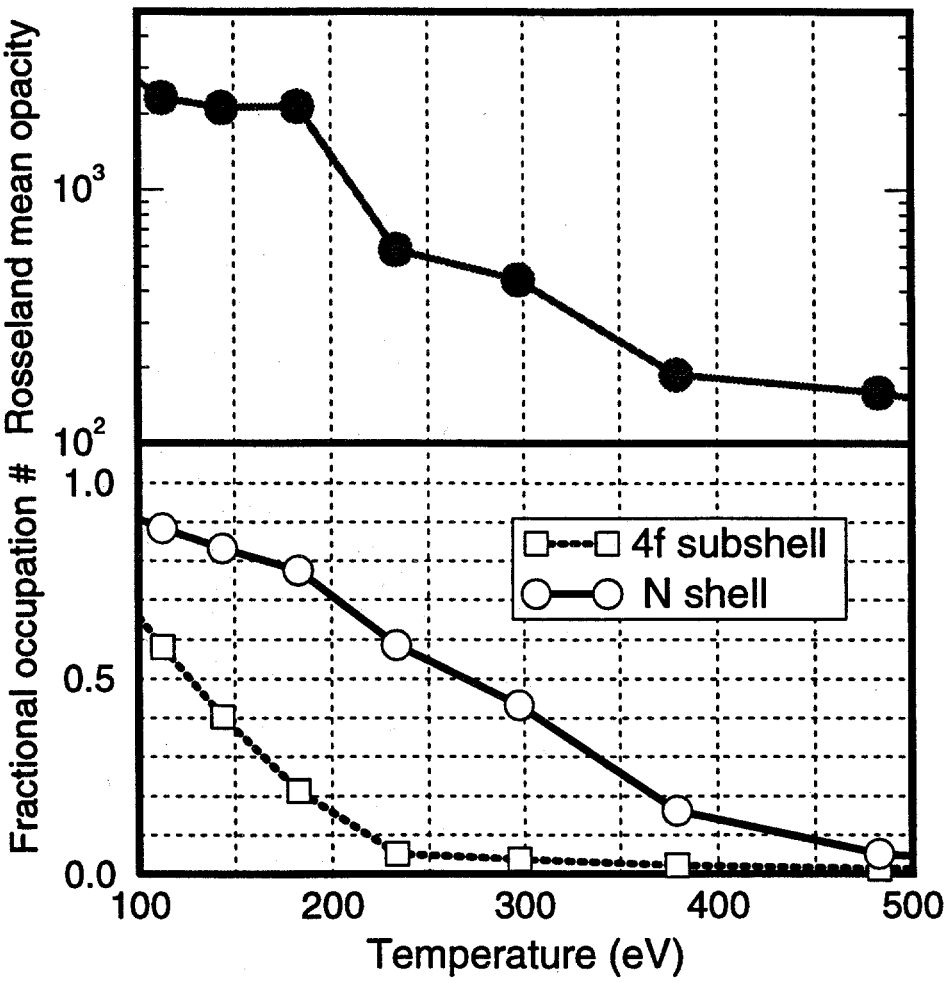

Figure 4. The effect of N shell electron population in Au on the Rosseland mean opacity. (Top) The Rosseland mean opacity for Au at a density of $\rho = 0.1$ g/cm^3. (Bottom) Fractional N shell electron population number, scaled to number of electrons of the closed shell.

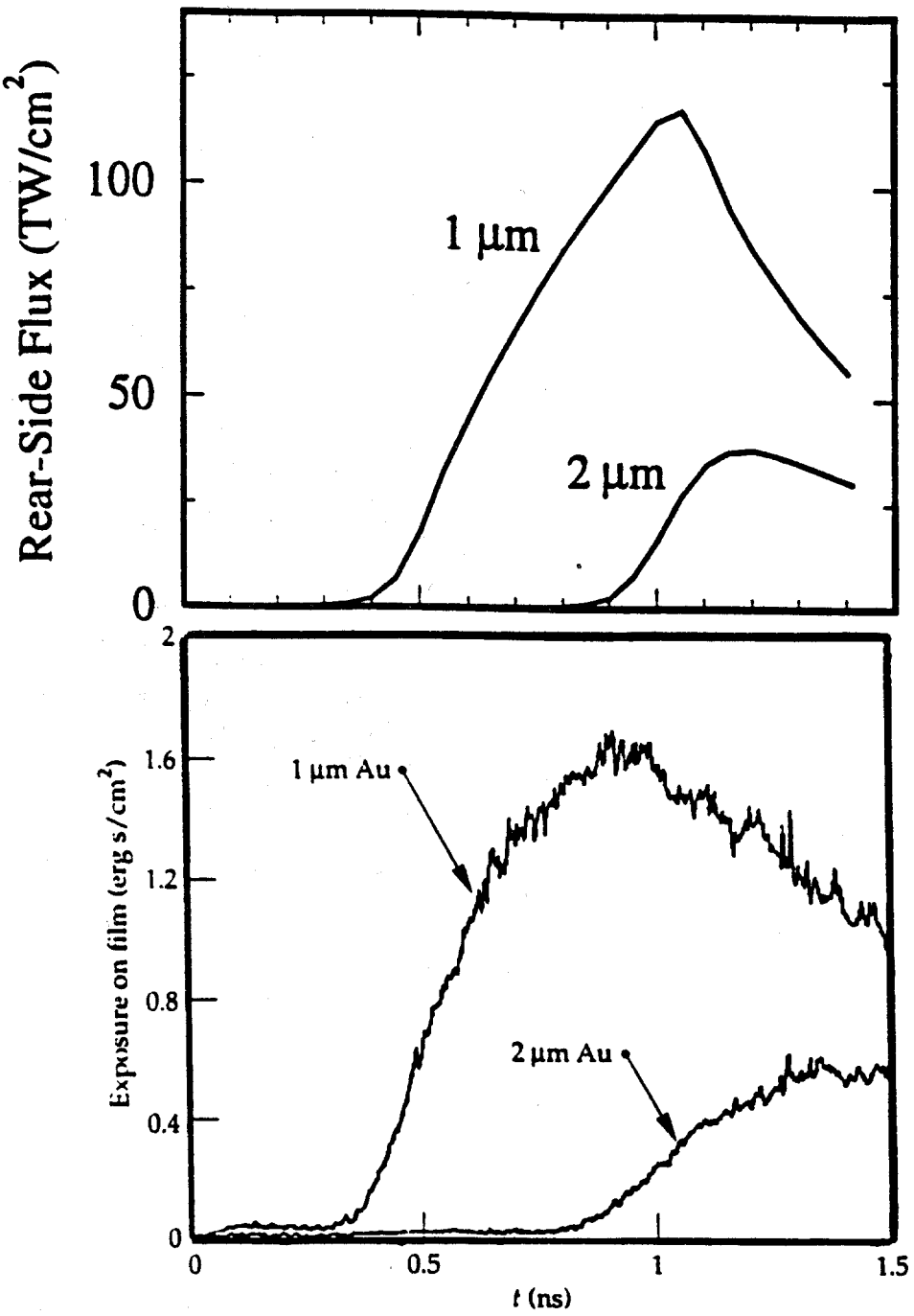

Figure 5. Comparison of the calculated rear side fluxes for 1 and 2 μm-thick foils (top) with experimental x-ray streak camera data (bottom[7]) of Au radiation burnthrough.